Composition dependence of the hydrostatic pressure coefficients of the bandgap of $ZnSe_{1-x}Te_x$ alloys

J. Wu,[1,2] W. Walukiewicz,[1,*] K. M. Yu,[1] W. Shan,[1] J. W. Ager III,[1] E. E. Haller,[1,2] I. Miotkowski,[3] A. K. Ramdas,[3] and Ching-Hua Su[4]

[1]*Materials Sciences Division, Lawrence Berkeley National Laboratory, Berkeley, California 94720, USA*
[2]*Department of Materials Science and Engineering, University of California, Berkeley, California 94720, USA*
[3]*Department of Physics, Purdue University, West Lafayette, Indiana 47907, USA*
[4]*SD46 Science Directorate, NASA/Marshall Space Flight Center, Huntsville, Alabama 35812, USA*

Optical absorption experiments were performed using diamond-anvil cells to measure the hydrostatic pressure dependence of the fundamental bandgap of $ZnSe_{1-x}Te_x$ alloys over the entire composition range. The first- and second-order pressure coefficients were obtained as a function of composition. The coefficients do not vary linearly between the ZnSe and ZnTe end-point values. Starting from the ZnSe side, the magnitude of both coefficients increases slowly until $x \approx 0.7$, which is the point where the ambient-pressure bandgap shows a minimum. At larger values of x the coefficients rapidly approach the values of ZnTe. The large deviations of the pressure coefficients from the linear interpolation between ZnSe and ZnTe are explained in terms of the band anticrossing model.

The nonlinear dependence of the bandgap energy with composition is a widely observed property of semiconductor alloys. In many semiconductor alloy systems, the deviation from a linear dependence can be described by a quadratic term proportional to the so-called bowing parameter (b). In this virtual crystal approximation (VCA) approach, bandgap bowing is explained by including effects of composition and structural disorder on the conduction and valence band edges.[1] The VCA works reasonably well for alloys of similar materials in which the bowing parameters are smaller or comparable to the bandgaps of the constituents.

Recently, a very strongly nonlinear composition dependence of the bandgap has been observed in highly electronegativity-mismatched group III-V nitride alloys such as $GaAs_{1-x}N_x$ (Refs. 2 and 3) and $InP_{1-x}N_x$.[4,5] It has been demonstrated that the composition dependence of the bandgap of these alloys cannot be described using a single bowing parameter.[6] In addition to the large bandgap bowing, a greatly reduced hydrostatic pressure dependence of the bandgap and a significant increase in the electron effective mass as compared to the end-point materials are also observed. The band anticrossing (BAC) model has been developed to explain these novel effects.[3,7] In the BAC model the anticrossing interaction between the previously observed resonant states of nitrogen and the conduction band states of the host semiconductor modifies the electronic structure and is responsible for the unusual properties of these alloys.

The BAC model has also been applied to highly mismatched group II-VI alloys including $ZnSe_{1-x}Te_x$ and $ZnS_{1-x}Te_x$, in which large bandgap bowings have also been observed.[8] The availability of group II-VI alloys covering the entire composition range provides an ideal opportunity to study the electronic structure of highly mismatched alloys. For example, it has been shown for $ZnSe_{1-x}Te_x$ alloys that on the ZnSe (ZnTe)-rich side, the bandgap bowing is mostly determined by an anticrossing interaction between the Te

(Se) localized level and the extended states of the ZnSe valence bands (ZnTe conduction band) near the Brillouin zone center.[8,9]

Here we report results of studies of the hydrostatic pressure dependence of the bandgap of $ZnSe_{1-x}Te_x$ alloys over the entire composition range. The results show an entirely different pressure dependence of the band gaps of ZnSe- and ZnTe-rich alloys. The behavior can be well explained by the anticrossing interaction between localized Se or Te levels and the extended states of the host semiconductor matrix.

Bulk $ZnSe_{1-x}Te_x$ single crystals were grown by either a modified Bridgman method[10] on the Te-rich side, or by the physical vapor transport method[11] on the Se-rich side. The samples were mechanically polished into small chips $\sim 100 \times 100 \ \mu m^2$ in size and a thickness of $\sim 10 \ \mu m$, and mounted into gasketed diamond anvil cells for the application of hydrostatic pressure. The pressure medium was a mixture of ethanol and methanol (1:4). The applied pressure was calibrated by the standard method of monitoring the red shift of the ruby $R1$ photoluminescence line. The optical absorption measurements were performed at room temperature using a 0.5 m single-grating monochromator and an ultraviolet-sensitive silicon photodiode as the detector.

Figure 1 shows the optical absorption curves of $ZnSe_{0.91}Te_{0.09}$ measured over a range of hydrostatic pressures. The apparent absorption below the band edge originates from the fact that the reflection of the beam from the surface of the sample has been neglected in the absorbance calculation. The curve at the top is a photomodulated reflectance (PR) spectrum taken at ambient pressure. The feature at lower energy corresponds to the critical transition from the top of the valence bands to the conduction band edge. The feature at higher energy is attributed to the transition from the top of the spin-orbit split-off valence band to the conduction band edge. The fundamental bandgap energy (E_g) determined from the PR spectrum 2.45 ± 0.06 eV is in good
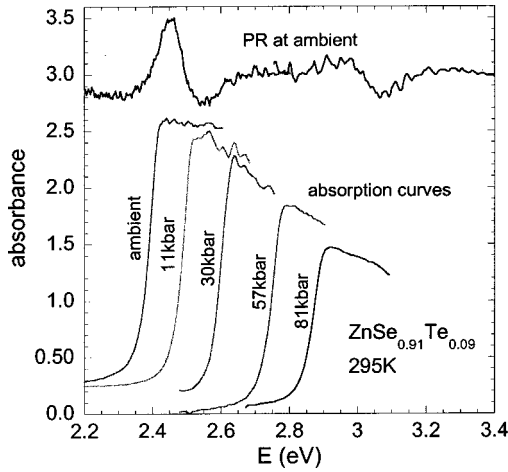
FIG. 1. Absorption curves of ZnSe$_{0.91}$Te$_{0.09}$ for a range of hydrostatic pressures. The curve at the top portion of the figure are photomodulated reflectance (PR) data taken at ambient pressure. All experiments were performed at room temperature.

agreement with the gap energy defined by the crossing point at 2.42 eV of the steeply rising portion and the saturation line of the ambient-pressure absorption curve.

The fundamental bandgap determined from the absorption curves shown in Fig. 1 is plotted as a function of pressure in Fig. 2. For a comparison, the pressure dependencies at several other compositions are also shown, including the end-point materials ZnSe and ZnTe. The measured pressure dependencies of ZnSe and ZnTe shown in Fig. 2 are in quantitative agreement with previous observations.[12,13] It can be seen from Fig. 2 that the bandgap of ZnTe shows a much more pronounced nonlinear behavior than the bandgap of ZnSe. This nonlinear behavior of the bandgap of semiconductors is typically attributable to the pressure dependence of the bulk modulus.
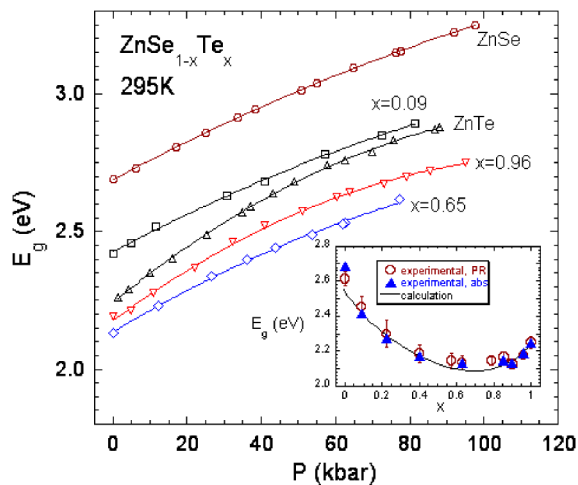

FIG. 2. Bandgap as a function of pressure for several compositions. The solid curves are quadratic fits to these data points using Eq. (1). Inset, ambient-pressure bandgap measured by PR and optical absorption experiments plotted as a function of composition. The curve is the calculated dependence based on the BAC model (Ref. 9).
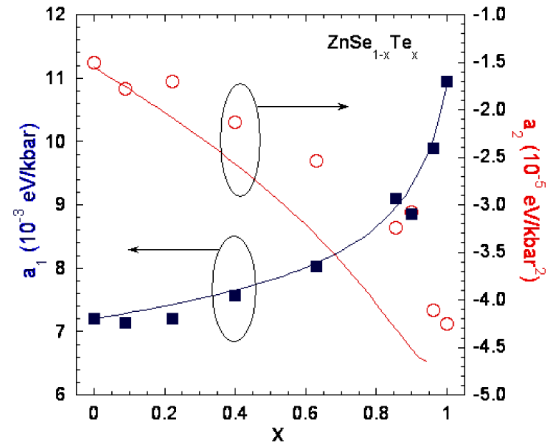

FIG. 3. Linear and second-order pressure coefficients as a function of composition. The curves are calculated coefficients based on the BAC model.

It is interesting to note an entirely different effect of alloying on the pressure dependence of the bandgaps of ZnSe- and ZnTe-rich alloys. Results in Fig. 2 show that ZnTe alloyed with only 4% of ZnSe shows a considerably weaker pressure dependence than ZnTe. On the other hand, the pressure dependence of the bandgap does not vary much with composition in ZnSe-rich alloys.

To quantitatively describe this nonlinear composition dependence of the pressure behavior of the bandgaps over the whole composition range $0 \leq x \leq 1$, we fit the pressure data of all samples with a quadratic equation

$$E_g(x,P) = E_g(x) + a_1(x)P + a_2(x)P^2, \tag{1}$$

where $E_g(x)$ is the composition-dependent bandgap at ambient pressure. The linear pressure coefficient $a_1(x)$ and the second-order pressure coefficient $a_2(x)$ can be obtained as a function of composition from the least-squared fitting using Eq. (1). Examples of numerical fits to the experimental data are shown by solid curves in Fig. 2.

The composition dependence of the bandgap at ambient pressure measured by both PR and optical absorption is shown in the inset of Fig. 2. The bandgap shows a convex dependence on the composition and reaches a minimum at $x \approx 0.7$. The solid curve represents the results of theoretical calculations based on the BAC model as described in Ref. 9. At ambient pressure the bandgap is given by the equation[9]

$$E_g(x) = (1-x)E_g^{\text{Se-rich}}(x) + xE_g^{\text{Te-rich}}(x), \tag{2}$$

where $E_g^{\text{Se-rich}}(x)$ is the bandgap calculated from the valence band edge shifted by the interaction with the localized levels of Te on the Se-rich side, and $E_g^{\text{Te-rich}}(x)$ is the bandgap calculated from the conduction band edge shifted by the interaction with the localized levels of Se on the Te-rich side.

The measured pressure coefficients are shown as a function of x in Fig. 3. The linear coefficient of ZnTe is 60% larger than that of ZnSe, and the second-order coefficient of ZnTe is three times larger than that of ZnSe. As demonstrated in Fig. 3, however, the pressure coefficients deviate signifi-

cantly from a simple linear interpolation between ZnSe and ZnTe. Starting from ZnSe, both a_1 and $|a_2|$ increase slowly until $x \sim 0.7$. After $x \sim 0.7$, they make a rapid transition to the values of ZnTe. The crossover of the changing rate near $x = 0.7$ corresponds to the composition at which $E_g(x)$ reaches its minimum. This behavior is in stark contrast with that of well-matched group II-VI alloys, such as $Zn_xCd_{1-x}Se$, in which a small bowing parameter ($b = 0.35$ eV) of the bandgap and a linear composition dependence of the pressure coefficients have been observed.[14]

The experimentally determined composition dependence of the pressure coefficients can be explained using the BAC model. In Te-rich alloys (x close to 1), the BAC model predicts a new conduction band edge formed by the anticrossing interaction between the Se localized states and the Γ conduction band of ZnTe.[8] The localized Se level lies 0.6 eV above the conduction band edge of ZnTe. It has been shown[8] that the perturbation of the Se localized states on the ZnTe conduction band successfully explains the composition and hydrostatic pressure dependencies of the fundamental bandgap on the Te-rich side. The conduction band edge of ZnTe rises rapidly with increasing pressure as can be seen from the data of ZnTe in Fig. 2. However, as is commonly known for localized states in semiconductors, their energy levels are insensitive to applied hydrostatic pressure due to the localized nature of their wave functions.[15] As the pressure increases, the conduction band edge of ZnTe moves up closer to the Se level, leading to a more localized nature of the hybridized wave function. As a result the rate of the bandgap energy increase is reduced. With further increase in pressure ($> \sim 100$ kbar), the conduction band edge states start to change in nature from extended-like to localized-like. Eventually the pressure dependence of the bandgap will approach the pressure behavior of the Se localized level, rising at the small rate of ~ 1.5 meV/kbar.[8,16]

For Se-rich alloys (x close to 0), the hybridization between the localized Te level and the valence bands of the host ZnSe has been shown to be responsible for the composition dependence of the bandgap and the spin-orbit splitting.[9] The Te deep level is located at ~ 0.1 eV above the valence band edge of ZnSe. As opposed to the effect on the Te-rich side, the hybridization with the valence bands does not significantly change the pressure behavior of the bandgap, because the conduction band states that are responsible for the pressure effects of the bandgap are not affected by the hybridization. The slow increase in the pressure coefficients with increasing x, is therefore attributed to two effects: the VCA effect that is a linear interpolation between ZnSe and ZnTe, and the negative contribution from the pressure-induced rise of the valence band edge that is Te localized level-like. These two effects tend to cancel each other, so that the pressure coefficients stay almost constant for small x, as is seen in Fig. 3.

In order to explain the experimental data over the entire composition range ($0 \leq x \leq 1$), we use Eq. (2) to find the first- and second-order pressure coefficients. Substituting pressure dependencies of the band states and the localized levels into Eq. (2), differentiation of Eq. (2) with respect to pressure gives rise to the calculated pressure coefficients as a function of composition. The calculated linear pressure coefficient as a function of composition is shown as a solid curve in Fig. 3. A very good agreement is obtained between the calculated $a_1(x)$ and experimental results. The calculated second-order coefficient $a_2(x)$ deviates from experimental data, especially on the Te-rich side. This is due to the fact that higher-order coefficients make considerable contributions to the pressure dependence of the bandgap that is calculated by solving the eigenvalues of the Hamiltonian matrices given by the BAC model.[9] We note that in the calculations no adjustable parameters have been used. All the parameters, such as the locations of the Te and Se levels and the interaction constants between the localized level and the band states, use the values that have been determined previously by fitting with bandgap bowing measurements. The results demonstrate that the BAC model provides a comprehensive description of the composition and the pressure dependencies of the fundamental bandgap of $ZnSe_{1-x}Te_x$. These dependencies can be decomposed into the VCA effect from the random alloying, and the BAC effect due to the hybridization between the localized levels associated with the minority component and the extended states of the majority component. The concurrence of the minimum of $E_g(x)$ and the drastic changes in $a_1(x)$ and $a_2(x)$ at $x \sim 0.7$ indicates the crossover from the composition region where the valence BAC dominates to that in which the conduction BAC dominates.

In summary, we have measured the hydrostatic pressure dependence of the bandgap of $ZnSe_{1-x}Te_x$ alloys over the entire composition range. Both the first-order and the second-order pressure coefficients as a function of composition show an abrupt change in slope around $x \sim 0.7$. This behavior correlates with the bowing effect of the bandgap which reaches a minimum also near $x \approx 0.7$. We have demonstrated that the pressure dependence can be decomposed into a random alloying effect and a nonlinear effect due to the band anticrossing interaction between the localized states and the band states in the alloy.

*Electronic address: w_walukiewicz@lbl.gov

[1] J. A. VanVechten and T. K. Bergstresser, Phys. Rev. B **1**, 3351 (1970); R. Hill and D. Richardson, J. Phys. C **4**, L289 (1971).

[2] M. Weyers, M. Sato, and H. Ando, Jpn. J. Appl. Phys. **31**, L853 (1992).

[3] W. Shan, W. Walukiewicz, J. W. Ager III, E. E. Haller, J. F. Geisz, D. J. Friedman, J. M. Olson, and S. R. Kurz, Phys. Rev. Lett. **82**, 1221 (1999).

[4] W. G. Bi and C. W. Tu, J. Appl. Phys. **80**, 1934 (1996).

[5] K. M. Yu, W. Walukiewicz, J. Wu, J. W. Beeman, J. W. Ager III, E. E. Haller, W. Shan, H. P. Xin, C. W. Tu, and M. C. Ridgway, J. Appl. Phys. **90**, 2227 (2001).

[6] U. Tisch, E. Finkman, and J. Salzman, Appl. Phys. Lett. **81**, 463 (2002).

[7] J. Wu, W. Shan, and W. Walukiewicz, Semicond. Sci. Technol. **17**, 860 (2002).

[8] W. Walukiewicz, W. Shan, K. M. Yu, J. W. Ager III, E. E. Haller, I. Miotkowski, M. J. Seong, H. Alawadhi, and A. K. Ramdas, Phys. Rev. Lett. **85**, 1552 (2000).

[9] J. Wu, W. Walukiewicz, K. M. Yu, J. W. Ager III, E. E. Haller, I. Miotkowski, A. K. Ramdas, Ching-Hua Su, I. K. Sou, R. C. C. Perera, and J. D. Denlinger, Phys. Rev. B **67**, 035207 (2003).

[10] M. J. Seong, H. Alawadhi, I. Miotkowski, A. K. Ramdas, and S. Miotkowska, Phys. Rev. B **60**, R16 275 (1999).

[11] C. H. Su, S. Feth, S. Zhu, S. L. Lehoczky, and L. J. Wang, J. Appl. Phys. **88**, 5148 (2000).

[12] K. Strossner, S. Ves, C. K. Kim, and M. Cardona, Solid State Commun. **61**, 275 (1987).

[13] S. Ves, K. Strossner, N. E. Christensen, C. K. Kim, and M. Cardona, Solid State Commun. **56**, 479 (1985).

[14] W. Gebhardt and G. Schtöz, in *Properties of Wide Bandgap II-VI Semiconductors*, edited by Rameshwar Bhargava, No. 17 of *EMIS Datareviews Series* (Institution of Electrical Engineers, London, 1997).

[15] J. M. Langer and H. Heinrich, Phys. Rev. Lett. **55**, 1414 (1985).

[16] J. Wu, W. Walukiewicz, K. M. Yu, J. W. Ager III, E. E. Haller, I. Miotkowski, A. K. Ramdas, and S. Miotkowska, Appl. Phys. Lett. **80**, 34 (2002).